

Minerva Access is the Institutional Repository of The University of Melbourne

Author/s:

Nam, E;Kim, J;Guntari, SN;Seyler, H;Fu, Q;Wong, EHH;Blencowe, A;Jones, DJ;Caruso, F;Qiao, GG

Title:

Continuous assembly of polymers via solid phase reactions

Date:

2014-01-01

Citation:

Nam, E., Kim, J., Guntari, S. N., Seyler, H., Fu, Q., Wong, E. H. H., Blencowe, A., Jones, D. J., Caruso, F. & Qiao, G. G. (2014). Continuous assembly of polymers via solid phase reactions. *Chemical Science*, 5 (9), pp.3374-3380. <https://doi.org/10.1039/c4sc01240b>.

Persistent Link:

<https://hdl.handle.net/11343/197470>



## Continuous Assembly of Polymers via Solid Phase Reactions

Journal:	<i>Chemical Science</i>
Manuscript ID:	SC-EDG-04-2014-001240.R1
Article Type:	Edge Article
Date Submitted by the Author:	22-May-2014
Complete List of Authors:	<p>Qiao, Greg; The University of Melbourne, Chemical and Biomolecular Engineering</p> <p>Nam, Eunhyung; The University of Melbourne, Chemical and Biomolecular Engineering</p> <p>Kim, Jinguik; The University of Melbourne, Chemical and Biomolecular Engineering</p> <p>Guntari, Stefanie Nina; The University of Melbourne, Chemical and Biomolecular Engineering</p> <p>Seyler, Helga; University of Melbourne, Chemistry/Bio21</p> <p>Fu, Qiang; The University of Melbourne, Chemical and Biomolecular Engineering</p> <p>Wong, Edgar; The University of Melbourne, Chemical and Biomolecular Engineering</p> <p>Blencowe, Anton; The University of Melbourne, Chemical and Biomolecular Engineering</p> <p>Jones, David; University of Melbourne, Chemistry/Bio21</p> <p>Caruso, Frank; The University of Melbourne, Chemical and Biomolecular Engineering</p>

## Continuous Assembly of Polymers via Solid Phase Reactions

*Eunhyung Nam,<sup>1</sup> Jinguk Kim,<sup>1</sup> Stefanie N. Guntari,<sup>1</sup> Helga Seyler,<sup>2</sup> Qiang Fu,<sup>1</sup> Edgar H. H. Wong,<sup>1</sup> Anton Blencowe,<sup>3</sup> David J. Jones,<sup>2</sup> Frank Caruso<sup>1\*</sup> and Greg G. Qiao<sup>1\*</sup>*

[1] E. Nam, J. Kim, Dr. S. N. Guntari, Dr. Q. Fu, Dr. E. H. H. Wong, Prof. F. Caruso, Prof. G. G. Qiao

Department of Chemical and Biomolecular Engineering,  
The University of Melbourne,  
Parkville, Victoria 3010 (Australia)

[2] Dr. H. Seyler, Dr. D. J. Jones  
School of Chemistry, Bio21 Institute,  
The University of Melbourne,  
30 Flemington Road, Parkville, Victoria 3010 (Australia)

[3] Dr. A. Blencowe  
Mawson Institute, Division of Information Technology, Engineering and the Environment,  
University of South Australia,  
Mawson Lakes, SA 5095 (Australia)

E-mail: gregghq@unimelb.edu.au

E-mail: fcaruso@unimelb.edu.au

Keywords: thin films, solid state, surface initiated polymerization, ring opening metathesis

### ABSTRACT

The continuous assembly of polymers in the solid state *via* ring-opening metathesis polymerization (ssCAP<sub>ROMP</sub>) is reported as an effective method for the fabrication of smooth, surface confined, cross-linked nanostructured films. Macrocross-linkers, polymers pre-functionalized with polymerizable pendent groups, were first deposited onto initiator-modified substrates via spin-coating, followed by film cross-linking via ssCAP<sub>ROMP</sub>. The film thickness is tunable by adjusting the reaction time, and multilayered films can be achieved through reinitiation steps, generating complex and unique film architectures with nanometer precision. The technique developed herein allows for controlled and directional growth of cross-linked thin films from the substrate surface in the solid state that is unlike any other conventional methods.

A number of approaches to fabricate cross-linked ultra thin films have been developed in recent decades, targeting a broad range of applications, including electronic devices,<sup>1-3</sup> membrane purification systems,<sup>4</sup> and biomaterials.<sup>5</sup> These include solution-based processes, such as grafting-from,<sup>6, 7</sup> grafting-to,<sup>8, 9</sup> and layer-by-layer (LbL) assembly,<sup>10-12</sup> where film formation generally occurs through the deposition of materials (e.g., monomers, macromolecules) from the solution state onto a solid substrate, followed by cross-linking of the film in a solvated state. Other widely employed techniques include spray or spin-coating,<sup>13, 14</sup> whereby preformed materials are firstly deposited onto a substrate, followed by cross-linking of the film in the solid state. Plasma polymerization at surfaces has also been widely employed to prepare cross-linked films in a single step.<sup>15-18</sup> In many cases, film cross-linking is essential to induce film stability, regardless of the approach employed (i.e., solution, solid, plasma state). There are several advantages of performing the cross-linking step in the solid state over the solution state. For instance, polymerization in the solid state usually results in higher molecular weight materials compared to solution state.<sup>19, 20</sup> Furthermore, the fabrication of homogeneous cross-linked films from highly rigid polymers with large molecular weights is extremely challenging using solution-based systems due to the inherent steric hindrance and diffusion barrier.<sup>21</sup> This issue is especially prominent for conjugated polymers employed in electronic devices as they generally have poor processability and possess rigid rod-like conformations.<sup>22, 23</sup>

Recently, we developed a film fabrication technology termed continuous assembly of polymers (CAP)<sup>24-27</sup> that involves the one-step assembly of (bio)polymers containing polymerizable pendant groups (defined as macrocross-linkers) to generate surface-confined, cross-linked nanoscale films. The CAP approach utilizes controlled chain-growth polymerization methodologies such as ring-opening metathesis polymerization (ROMP),<sup>28</sup> atom transfer radical polymerization (ATRP),<sup>29, 30</sup> and photoiniferter-mediated

polymerization<sup>31, 32</sup> to cross-link macrocross-linkers from initiator-functionalized substrates, resulting in controlled and tunable film properties. Our previous studies have so far centered on building functional and compositionally complex (multilayered) films on planar and colloidal substrates where film cross-linking solely occurs in the solution state.<sup>33, 34</sup> However, limited success was attained in assembling films from polymers with high molecular weights and rigid conformations.<sup>35</sup> Herein, we broaden the scope of the CAP technique by developing solid state CAP (ssCAP). Using a rigid regioregular poly(3-hexylthiophene)<sup>36, 37</sup> (P3HT)-based macrocross-linker as a model polymer, the viability of the ssCAP approach is demonstrated. The introduced ssCAP is distinctive from conventional cross-linking strategies in the solid state. Whereas other solid state cross-linking techniques occur in a step growth manner (i.e., the step-by-step addition between molecules/polymers of complementary functionalities) via thiol-ene or thiol-yne photopolymerizations<sup>38, 39</sup> for instance, ssCAP proceeds via a chain-growth mechanism from the substrate surface where cross-linked film networks are formed in a bottom-up direction. In essence, ssCAP allows for simultaneous directional growth and cross-linking of thin films that is difficult to achieve using currently available solid state methods.

In ssCAP, the macrocross-linker is firstly deposited onto an initiator-immobilized substrate (via spin-coating), followed by solvent evaporation and subsequent annealing above the glass transition temperature ( $T_g$ ) of the macrocross-linker to initiate the CAP process (**Figure 1**). The cross-linked film assembly step via ssCAP occurs under solvent-free conditions. Since the macrocross-linker is deposited onto the substrate via spin-coating prior to the CAP process, there is potentially no limitation for the type of solvent, the molecular weight as well as the conformation of the polymer used in ssCAP, overcoming issues associated with steric and diffusion barriers normally encountered in solution-based CAP systems. In this study, ring-opening metathesis polymerization (ROMP) was chosen as the controlled polymerization

technique of choice to mediate the ssCAP reaction ( $\text{ssCAP}_{\text{ROMP}}$ ). ROMP is a most widely used polymerization methodology to synthesize well-defined polymers due to its versatility and high functional-group tolerance, allowing mild reaction conditions, short reaction times, and the use of a wide range of monomers.<sup>40</sup> Furthermore, ROMP can be performed in bulk without the presence of solvents, for example, in applications such as self-healing polymeric materials<sup>41,42</sup> and clay exfoliation using dicyclopentadiene.<sup>43</sup>

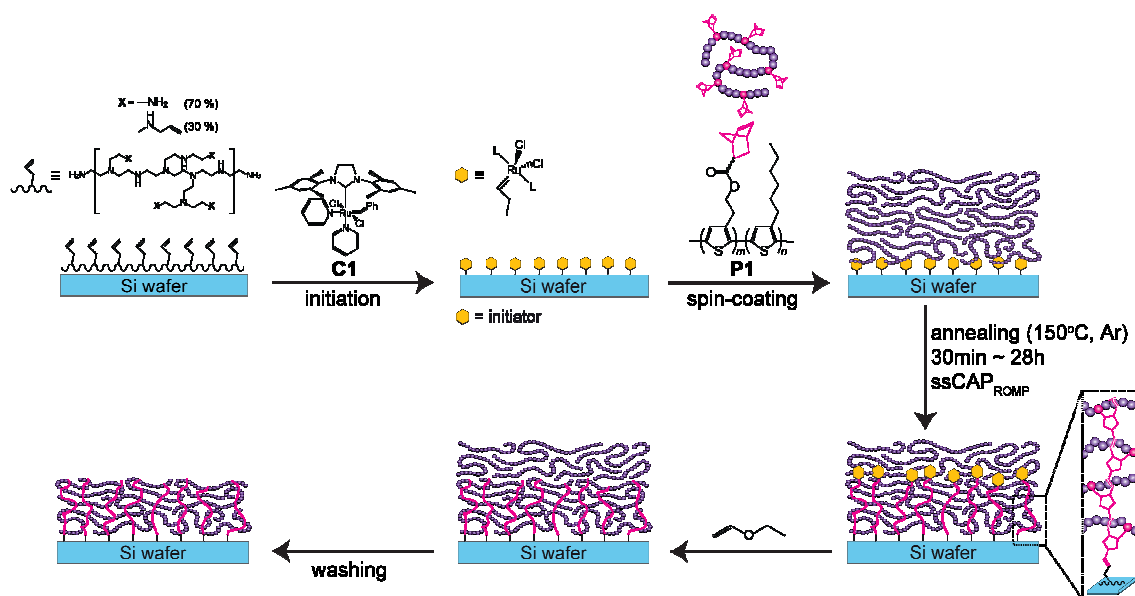


**Figure 1.** General scheme for solid state  $\text{CAP}_{\text{ROMP}}$ .

Film fabrication via  $\text{ssCAP}_{\text{ROMP}}$  was performed on Si wafers, which were modified with a monolayer of allyl-modified poly(ethylene imine) (allyl-PEI) followed by the immobilization of ruthenium (Ru) catalyst **C1** (pyridine modified 2<sup>nd</sup> generation Grubbs catalyst)<sup>44</sup> to generate initiator-functionalized surfaces (**Figure 1**). The preformed P3HT<sup>36, 37</sup>-based macrocross-linker **P1** containing 13.5 mol% of pendent polymerizable norbornene groups was spin-coated onto the initiator-functionalized substrate to afford a 150 nm thick film, which was annealed under an argon atmosphere at 150 °C to facilitate polymerization and effect the  $\text{ssCAP}_{\text{ROMP}}$  process. After a predetermined time, the reaction was ceased by removing the Ru

catalyst from the system by addition of ethyl vinyl ether,<sup>28</sup> and the substrate was washed thoroughly with chloroform to remove any non-cross-linked polymer prior to analysis.

Film thicknesses and the surface roughness (as indicated by the root mean square (rms) values) of **P1** ssCAP films prepared at different polymerization times were determined using AFM (**Figure 2a**). The film thickness was found to increase with annealing time, before reaching a plateau at *ca.* 70 nm after 15 h of polymerization. Cessation of cross-linking is most likely attributed to the propagating groups becoming spatially isolated and restricted within the cross-linked portion of the film, and thus not being within distance of other cross-linkable moieties. In addition, the steric congestion at these spatially isolated sites could also prevent the diffusion of uncross-linked macrocross-linkers from reaching the propagating groups. The resulting films have a fairly constant surface roughness throughout the polymerization time, with rms values ranging from 1.5 to 3.5 nm (**Figure 2b**). In comparison to CAP<sub>ROMP</sub> reactions performed in solution, whereby the generated CAP films typically have rms values between 49 to 67 nm,<sup>21, 32</sup> ssCAP<sub>ROMP</sub> generates significantly smoother cross-linked films (although the type of polymer may also have an influence on the resulting film coverage). In ssCAP<sub>ROMP</sub>, a smooth layer of film is evenly pre-coated onto a substrate by spin-coating prior to cross-linking reactions. This ensures that a homogeneous layer of non-cross-linked film is formed before subsequent ssCAP<sub>ROMP</sub> reactions. This is distinguishable from solution-based CAP processes where film homogeneity depends on the diffusion of randomly dispersed macrocross-linkers in solution towards the reactive surface, and hence does not necessarily yield a smooth surface coating. A control experiment performed at 150 °C in the absence of catalyst **C1** indicates negligible formation of a cross-linked film, with a film thickness of *ca.* < 10 nm (inclusive of *ca.* 3 nm of allyl-PEI initiator monolayer) (Figure S1 in Supporting Information, SI). The control experiment crucially demonstrates that film cross-linking is mediated by surface-initiated ROMP and does not result from self-

polymerization of the pendent norbornene groups at high temperature. The effect of polymerization temperature in ssCAP<sub>ROMP</sub> was also investigated. Reactions performed at 80 and 25 °C (i.e., below the  $T_g$  of macrocross-linker **P1**)<sup>45</sup> showed negligible film growth, similar to that of the control experiment (Figure S2, SI). It is postulated that the macrocross-linker **P1**, which is crystalline in nature, attains a higher flexibility and mobility in the solid state when annealed above its  $T_g$ , thereby making the pendent norbornene groups more accessible to propagating Ru catalysts.

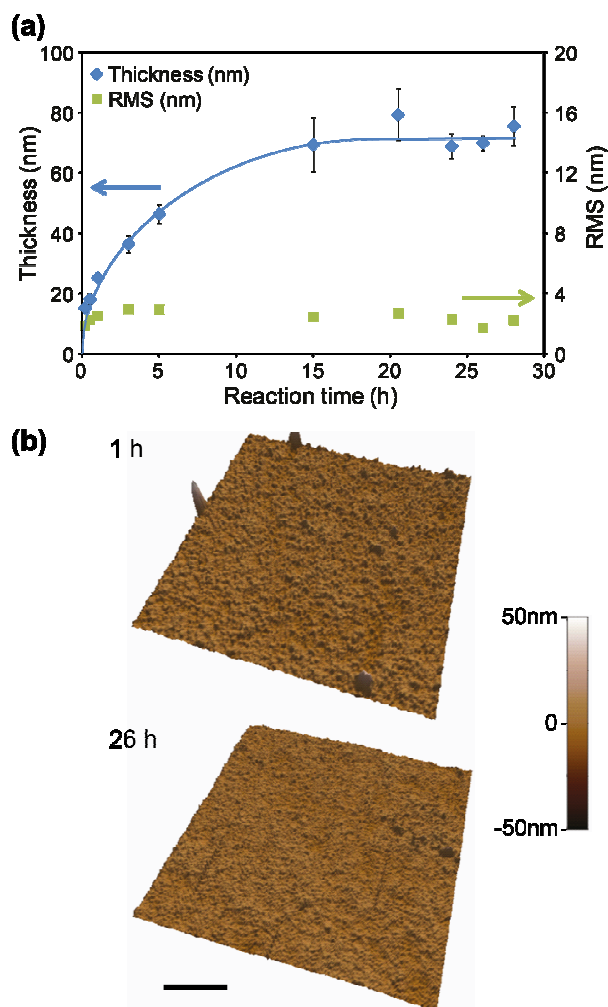


**Figure 2.** a) Thickness and surface roughness of **P1** films fabricated via ssCAP<sub>ROMP</sub> as a function of polymerization time. b)  $5 \times 5 \mu\text{m}$  3D height mode AFM images of **P1** films (1 and 26 h). Scale bar =  $1 \mu\text{m}$ .

Subsequently, the efficiency of ssCAP<sub>ROMP</sub> with respect to different spin-coated film thicknesses containing macrocross-linker **P1** was investigated. Various concentrations of **P1** (10 to 30 mg.mL<sup>-1</sup> in chloroform) were spin-coated onto initiator-functionalized substrates under identical spin-coating conditions (2000 rpm, 33 s) to obtain different film thicknesses (49, 107, 150, 201 and 240 nm), as determined by AFM. The films were subsequently annealed at 150 °C for 24 h under argon to allow for polymerization and film cross-linking via ssCAP<sub>ROMP</sub>. After thorough washing with chloroform to remove non-cross-linked polymer, the CAP efficiency was calculated as the ratio of the final film thicknesses after ssCAP<sub>ROMP</sub> relative to the original spin-coated film thicknesses prior to cross-linking.

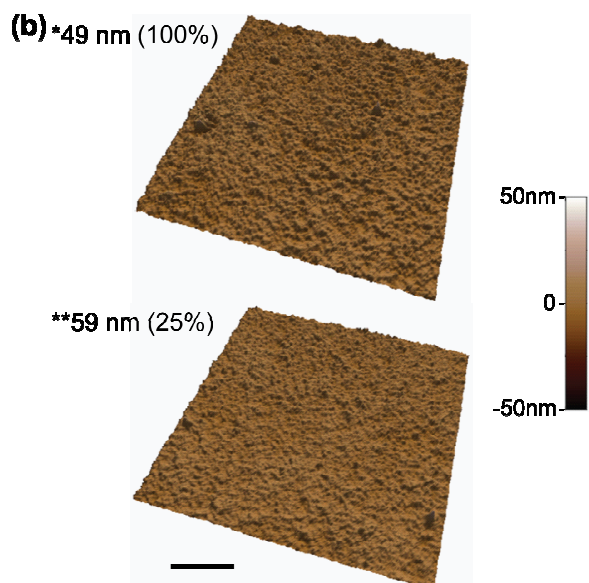
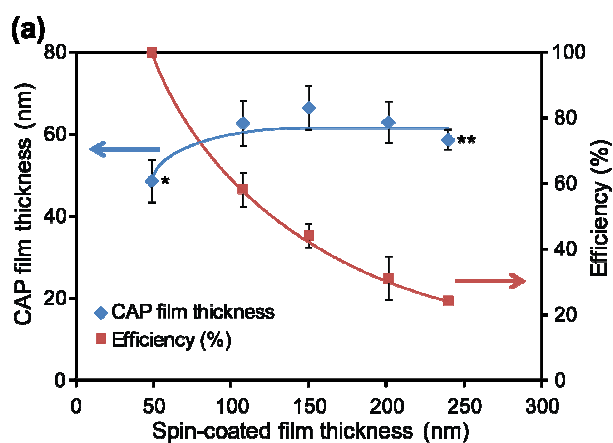


**Figure 3. a) Thicknesses of P1 CAP films and CAP efficiencies as a function of different spin-coated film thicknesses. b)  $5 \times 5 \mu\text{m}$  3D height mode AFM images of CAP films formed with different CAP efficiencies. Scale bar =  $1 \mu\text{m}$ .**

**Figure 3a** shows the final **P1** CAP film thicknesses and the calculated CAP efficiencies at different spin-coated film thicknesses. At a **P1** concentration of  $10 \text{ mg mL}^{-1}$  and spin-coated film thickness of 49 nm, both the original spin-coated and cross-linked CAP films showed an identical film thickness of 49 nm, yielding 100% CAP efficiency. However, the thickness of the cross-linked CAP films did not increase beyond 64 nm, even though the thickness of spin-coated films increased from 107 to 240 nm, resulting in a decrease in CAP efficiency. This indicates that the CAP film reaches a maximum and constant thickness of 64 nm under the conditions employed.

The applicability of  $\text{ssCAP}_{\text{ROMP}}$  to other types of macrocross-linkers was also investigated using a polyethylene glycol (PEG)-based macrocross-linker **P2** (**Figure 4a**), which was employed under similar conditions to those used for macrocross-linker **P1** except for a lower annealing temperature of  $25 \text{ }^\circ\text{C}$ . Low molecular weight PEGs such as macrocross-linker **P2** are amorphous in nature and have low  $T_g$  values ( $< 25 \text{ }^\circ\text{C}$ ) and therefore would have sufficient flexibility and mobility to undergo solid state polymerization even at room temperature. Spin-coated **P2** films were left to react at  $25 \text{ }^\circ\text{C}$  for 24 h under argon, followed by washing and sonication with isopropanol to remove any non-cross-linked polymers. The trend in CAP efficiencies for **P2** films at different spin-coated film thicknesses (*ca.* 17, 40 and 64 nm) were determined to be analogous to that of macrocross-linker **P1**.

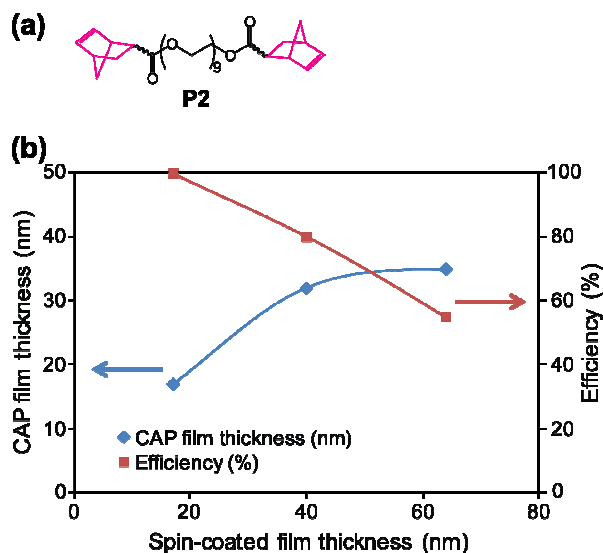


**Figure 4.** a) Chemical structure of PEG-based macrocross-linker **P2** used in  $ssCAP_{ROMP}$ . b) Thicknesses of **P2** CAP films and CAP efficiencies with respect to different spin-coated film thicknesses.

The resulting CAP film thicknesses and CAP efficiencies relative to the different spin-coated film thicknesses are presented in **Figure 4b**. Whereas 100% CAP efficiency was attained for films with a spin-coated thicknesses of 17 nm, the CAP efficiency decreased to 80 and 55% for 40 and 64 nm spin-coated film thicknesses, respectively, as the CAP film reached a maximum and constant thickness of 34 nm.

An attractive feature of  $CAP_{ROMP}$  films is the ability to resume film growth or layer extension via so-called ‘reinitiation’<sup>24, 33, 34</sup> steps. The unreacted pendent norbornene groups from the macrocross-linker in  $CAP_{ROMP}$  films serve as new initiating sites through post-functionalization with Ru catalysts, enabling the resumption of film growth via additional  $CAP_{ROMP}$  reactions. Similar to our previous studies in solution state  $CAP$ ,<sup>24, 33, 34</sup> new initiating sites are generated on  $ssCAP_{ROMP}$  films through cross-metathesis reactions between the terminal alkene on the surface of the film and the unreacted pendant norbornene groups in

the film with fresh Ru catalyst **C1**. For example, a **P1** CAP film (of thickness *ca.* 46 nm fabricated with 100 % CAP efficiency) was immersed in a solution of **C1** (4 mM in anhydrous DCM) for 30 min. During the immersion process in DCM, the cross-linked layer of film (denoted as L1) swells, thereby enabling the terminal alkenes on the surface and unreacted pendant norbornene groups in the film to undergo cross-metathesis reaction with fresh Ru catalyst **C1**. After rinsing and drying, macrocross-linker **P1** was spin-coated (10 mg.mL<sup>-1</sup>, 2000 rpm, 33 s) onto the reinitiated L1 surface to afford a spin-coated film thickness of *ca.* 59 nm (total film thickness of 105 nm), which was annealed at 150 °C for 24 h under argon to effect the successive ssCAP<sub>ROMP</sub> reaction, forming the second layer of cross-linked CAP film (L2) (**Figure 5a**). The process was repeated another three times to form multilayer films up until layer 5 (L5) and the increase in film thickness and change in surface topology after each reinitiation/CAP step was investigated via AFM analysis. **Figure 5b** illustrates a consistent increase in film thickness by *ca.* 59 nm after each reinitiation/CAP step (i.e., 100 % CAP efficiency), starting from *ca.* 46 nm for the first CAP layer (L1) to 283 nm after a total of five CAP reactions (L5). While the film thickness was found to increase linearly, the rms values remain < 5 nm from L1 to L5. Height profiles across the scratched zones of L1 to L5 obtained by AFM (**Figure 5c**) revealed a consistent increase in film thickness and uniform film formation with each layer extension. **Figure 5d** shows the 3D-height image of L1 and L3, which indicate a lack of change in surface topology between L1 (rms = 2.9 nm) and L3 (rms = 3.4 nm). It is worth noting that reinitiation in ssCAP<sub>ROMP</sub> is more efficient compared to solution-based CAP<sub>ROMP</sub>, which only generates a *ca.* 10 nm increase in film thickness per reinitiation step from an initial layer of *ca.* 120 nm. The higher layer extension efficiency in ssCAP<sub>ROMP</sub> is likely to result from denser films as compared to films made via CAP<sub>ROMP</sub> in solution. Although the amount of polymerizable groups may be the same for any given macrocross-linker, the density of these functional groups would be different depending on the overall film density. Hence, for denser films made via ssCAP<sub>ROMP</sub>, the amount of unreacted

norbornene and terminal alkene groups within and on the surface may be higher compared to lower density films. That is, there are more initiating sites available in ssCAP<sub>ROMP</sub> films than solution-based CAP<sub>ROMP</sub> films to promote subsequent layer extension reactions more effectively. In addition, the smooth and homogeneous topology of the ssCAP<sub>ROMP</sub> films (rms < 5 nm) could also play a role in exposing new initiating sites more effectively than the rougher topology of solution-based CAP<sub>ROMP</sub> film (rms = 49 to 67 nm) after the reinitiation, making the initiators more accessible towards reaction with the polymerizable groups of the macrocross-linker.

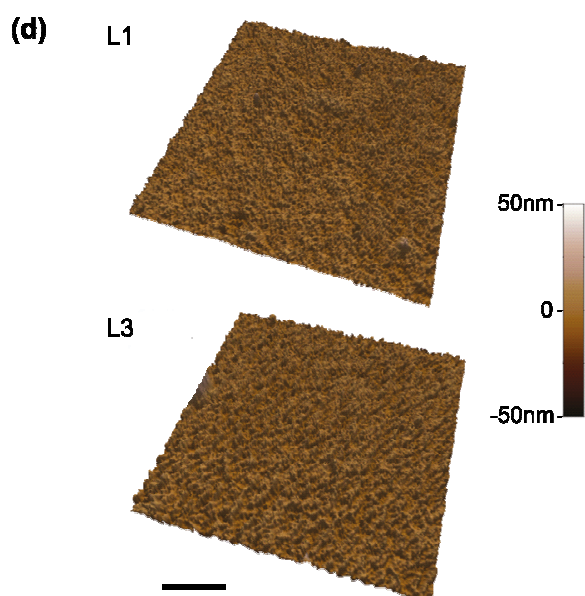
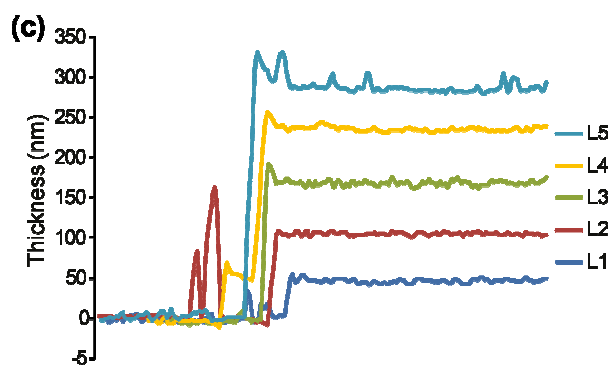
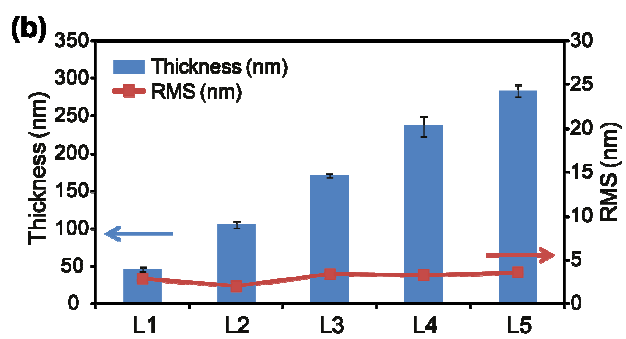
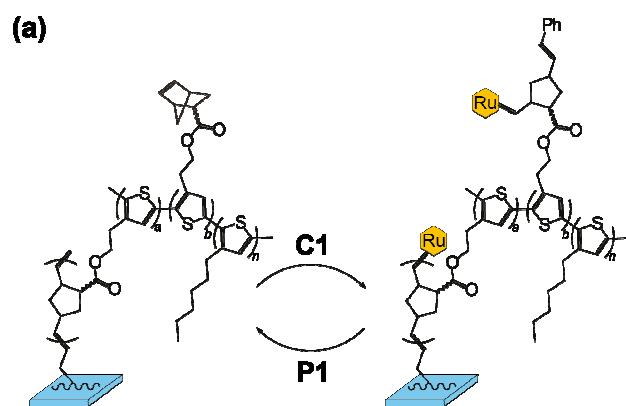


**Figure 5. a) General scheme showing the reinitiation of CAP films through addition of fresh Ru catalyst C1 and subsequent ssCAP<sub>ROMP</sub> with macrocross-linker P1. b) Plot of total film thicknesses with increasing reinitiation and CAP steps (defined as L layers), as measured by AFM. c) The z-profiles across the scratched zones of CAP<sub>ROMP</sub> films obtained after each reinitiation and CAP step, as measured by AFM. d) 5 × 5 μm 3D height mode CAP films of L1 and L3. Scale bar = 1 μm.**

As a result of improvements in film thickness after reinitiation, the CAP efficiency of the second P1 layer (L2) via ssCAP<sub>ROMP</sub> on top of an initial P1 CAP layer (L1) (*ca.* 50 nm) was investigated. Various thicknesses of spin-coated L2 layers (*ca.* 56, 132, 181, 230 and 283 nm) were prepared on identical L1 layers immobilized with fresh initiating sites, followed by the aforementioned ssCAP<sub>ROMP</sub> procedure. **Figure 6a** displays the L2 CAP film thicknesses and the corresponding CAP efficiencies based on various spin-coated L2 film thicknesses. **Figure 6a** reveals that high CAP efficiency of L2 (> 90%) was achieved for spin-coated film thicknesses up to 181 nm. The L2 CAP film thicknesses reached a maximum value of *ca.* 190 nm while the surface morphology remained the same (**Figure 6b**). The CAP efficiency of L2 films was found to be higher than that of L1 films. As mentioned previously, this most likely results from the higher surface density of initiating sites in L1 films compared to the initial monolayer of allyl-PEI primed onto the substrate.

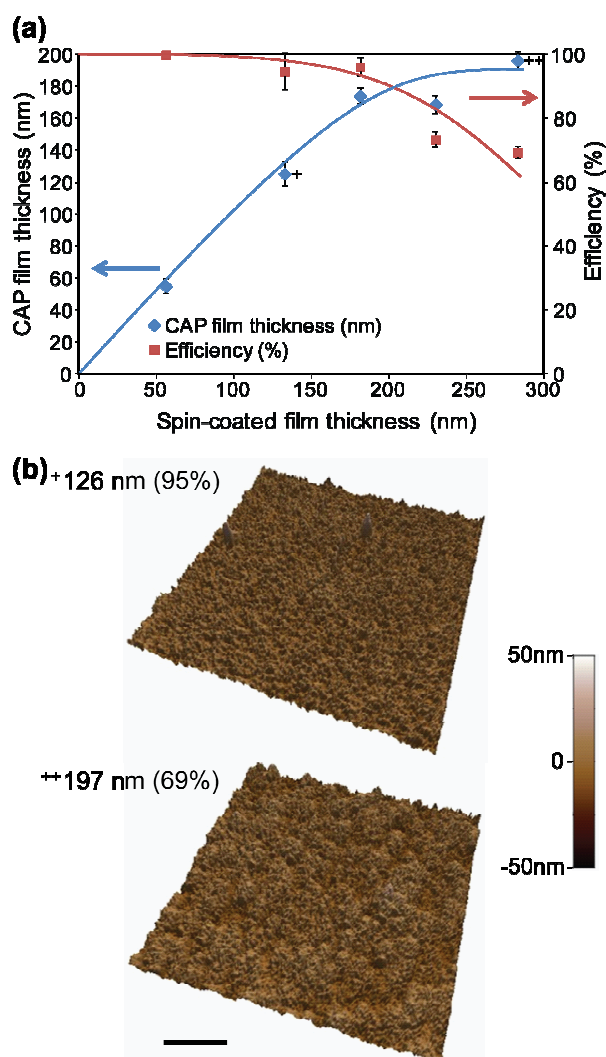


**Figure 6.** a) Second layer (L2) P1 CAP film thicknesses and CAP efficiencies with respect to different spin-coated film thicknesses. b)  $5 \times 5 \mu\text{m}$  3D height mode AFM images of CAP films formed at different CAP efficiencies. Scale bar =  $1 \mu\text{m}$ .

Reinitiation/layer extension is not only amenable to subsequent  $\text{CAP}_{\text{ROMP}}$  reactions but also to grafting-from processes to form polymer brush films. Using the grafting-from approach ROMP was implemented to fabricate polymer brushes on top of L1 P1 CAP films. Following the reinitiation step of attaching fresh Ru C1 catalysts as described previously, the substrate was exposed to norbornene M1 in solution or solidstate environments to generate poly(norbornene) brushes on the outer surfaces (**Figure 7a**). Grafting-from in the solution

state was conducted by immersing the L1-coated substrate in a solution of **M1** ( $10 \text{ mg.mL}^{-1}$  in DCM) for 24 h. For solid state polymerization, a solution of **M1** ( $50 \text{ }\mu\text{L}$ ,  $10 \text{ mg.mL}^{-1}$  in  $\text{CHCl}_3$ ) was spin-coated onto the L1 films (2000 rpm, 33 s) and annealed at  $150 \text{ }^\circ\text{C}$  for 24 h under an argon. The film thickness increased from 58 to 83 nm (an increment of 25 nm) for reactions conducted in the solution state whereas the reaction in solid state yielded a similar increase in film thickness of 18 nm (from 49 to 67 nm). **Figure 7b** presents 3D height mode AFM images of poly(norbornene) brushes generated in the solution and solid state, showing a significant difference in surface topology. The grafted film generated in the solution state has a pitted film morphology (rms = 3.5 nm) that is comparable to the polymer brushes formed via surface-initiated polymerization techniques.<sup>46, 47</sup> In comparison, films fabricated in the solid state are relatively smoother with no specific surface pattern (rms = 2.7 nm). This grafting-from experiment further demonstrates the versatility of  $\text{CAP}_{\text{ROMP}}$  films in fabricating multicompositional and structurally complex films that are distinctive to other methods. Noteworthy, Fourier transform IR (FTIR) experiments have been performed to determine the amount of norbornene groups left in the film after ssCAP. However, this was not possible due to the difficulty in distinguishing the C=C stretch of the unreacted norbornenes from those of the polynorbornene formed after ring opening reactions.

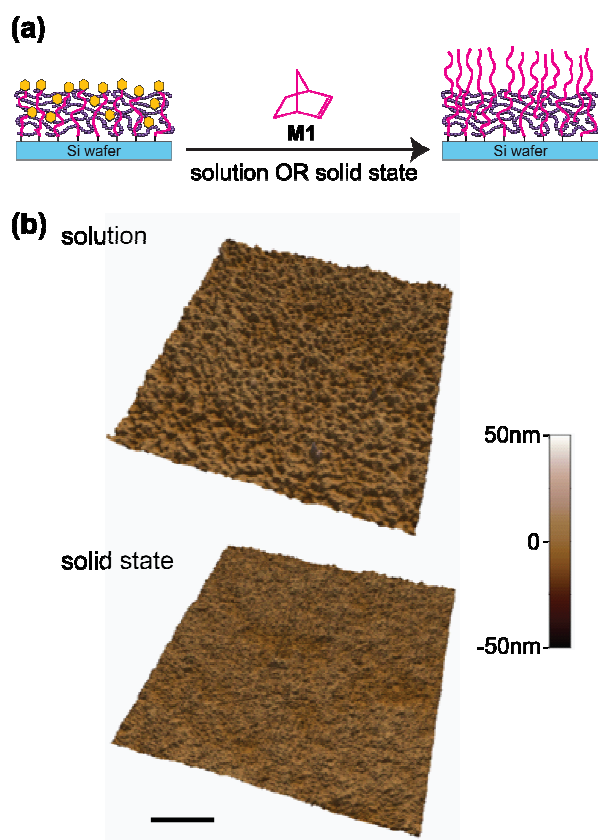


**Figure 7.** a) Reinitiation of P1 CAP films via grafting-from in solution or solid state using norbornene as the model monomer. b)  $5 \times 5 \mu\text{m}$  3D height mode AFM images of surface-grafted poly(norbornene) brushes generated by solution and solid state ROMP, respectively. Scale bar =  $1 \mu\text{m}$ .

In conclusion, a new film fabrication strategy,  $\text{ssCAP}_{\text{ROMP}}$ , based upon the combination of spin-coating and solid state polymerization was developed. This method allows for the efficient generation of cross-linked polymeric films with controllable film properties dictated by the polymerization time and the macrocross-linker concentration used in the spin-casting step. It was found that the reaction temperature must exceed the  $T_g$  of the macrocross-linker to effect the  $\text{ssCAP}_{\text{ROMP}}$  process. Films prepared by solid state  $\text{CAP}_{\text{ROMP}}$  reactions were found to be smoother compared to films made via solution state  $\text{CAP}_{\text{ROMP}}$ . Additionally, the generated CAP films are highly versatile, enabling resumption of film growth via reinitiation/layer

extension reactions through unreacted norbornene and terminal alkene groups within the films. Resumption of film growth can occur via either CAP or conventional grafting-from reactions. This unique feature of CAP<sub>ROMP</sub> films also allows for the generation of multilayered and structurally complex films via directional growth and simultaneous film cross-linking. The process can be repeated multiple times using the same or different macrocross-linkers. ssCAP<sub>ROMP</sub> can potentially be applied to a range of patterned and contoured surfaces. Current efforts are focused on applying the conductive polymer films as possible semiconductor devices and for potential biomedical and electronic applications.

### Experimental Section

*Assembly of solid state CAP<sub>ROMP</sub> films on planar substrates:* In a typical experiment, a Si wafer (*ca.* 1 cm x 1 cm) functionalized with catalyst **C1** (detailed functionalization procedures are provided in the SI) was spin-coated with a solution (50  $\mu$ L) of P3HT-based macrocross-linker **P1** in CHCl<sub>3</sub> (20 mg/mL, 2000 rpm, 33 s) and annealed at 150 °C under argon for a predetermined time to effect the ssCAP<sub>ROMP</sub> process. The ssCAP<sub>ROMP</sub> reaction was stopped by soaking the Si wafer in 5 mL of DCM solution containing 2% v/v ethyl vinyl ether to detach the Ru catalyst from the surface of the films. The polymer-coated wafer was washed thoroughly with and soaked in CHCl<sub>3</sub> (1 mL) for 12 h to remove any non-cross-linked polymers, and dried *in vacuo* prior to analysis. Multilayering was performed via repetition of the above procedure with intermediate reinitiation of the active norbornene sites (refer to SI for detailed procedures).

### Supporting Information

Supporting Information is available from the Wiley Online Library or from the authors.

### Acknowledgements

This work was supported by the Australian Research Council under the Australian Laureate Fellowship (FL120100030, F.C.), Future Fellowship (FT110100411, G.G.Q.), Discovery Project (DP1094147 and DP130101846, F.C., G.G.Q.) and Super Science Fellowship (FS110200025, Q.F. and G.G.Q.) schemes. E.N. and J.K. also acknowledge the receipt of an Australian Postgraduate Award (APA) and financial support through the CRC Program, respectively, from the Australian Government.

## References

1. K. T. Kamtekar, A. P. Monkman and M. R. Bryce, *Adv. Mater.*, 2010, **22**, 572-582.
2. M. Helgesen, R. Søndergaard and F. C. Krebs, *J. Mater. Chem.*, 2010, **20**, 36-60.
3. J. Y. Kim, K. Lee, N. E. Coates, D. Moses, T.-Q. Nguyen, M. Dante and A. J. Heeger, *Science*, 2007, **317**, 222-225.
4. M. M. Pendergast and E. M. Hoek, *Energy & Environmental Science*, 2011, **4**, 1946-1971.
5. E. Delamarche, A. Bernard, H. Schmid, A. Bietsch, B. Michel and H. Biebuyck, *J. Am. Chem. Soc.*, 1998, **120**, 500-508.
6. R. Barbey, L. Lavanant, D. Paripovic, N. Schüwer, C. Sugnaux, S. Tugulu and H.-A. Klok, *Chem. Rev.*, 2009, **109**, 5437-5527.
7. A. Olivier, F. Meyer, J.-M. Raquez, P. Damman and P. Dubois, *Prog. Polym. Sci.*, 2012, **37**, 157-181.
8. L. Huang, S. Dolai, K. Raja and M. Kruk, *Langmuir*, 2010, **26**, 2688-2693.
9. L. Nebhani, P. Gerstel, P. Atanasova, M. Bruns and C. Barner-Kowollik, *J. Polym. Sci., Part A: Polym. Chem.*, 2009, **47**, 7090-7095.
10. G. Decher, *Science*, 1997, **277**, 1232-1237.
11. J. F. Quinn, A. P. R. Johnston, G. K. Such, A. N. Zelikin and F. Caruso, *Chem. Soc. Rev.*, 2007, **36**, 707-718.
12. M. A. C. Stuart, W. T. S. Huck, J. Genzer, M. Muller, C. Ober, M. Stamm, G. B. Sukhorukov, I. Szleifer, V. V. Tsukruk, M. Urban, F. Winnik, S. Zauscher, I. Luzinov and S. Minko, *Nat Mater*, 2010, **9**, 101-113.
13. B. Harnish, J. T. Robinson, Z. Pei, O. Ramström and M. Yan, *Chem. Mater.*, 2005, **17**, 4092-4096.
14. D. Y. Ryu, K. Shin, E. Drockenmuller, C. J. Hawker and T. P. Russell, *Science*, 2005, **308**, 236-239.
15. H. Schreiber, M. Wertheimer and A. Wrobel, *Thin Solid Films*, 1980, **72**, 487-494.
16. H. Muguruma and I. Karube, *TrAC Trends in Analytical Chemistry*, 1999, **18**, 62-68.
17. X. Cheng, H. E. Canavan, M. J. Stein, J. R. Hull, S. J. Kweskin, M. S. Wagner, G. A. Somorjai, D. G. Castner and B. D. Ratner, *Langmuir*, 2005, **21**, 7833-7841.
18. A. Michelmores, D. A. Steele, J. D. Whittle, J. W. Bradley and R. D. Short, *RSC Advances*, 2013, **3**, 13540-13557.
19. S. Vouyiouka, E. Karakatsani and C. Papaspyrides, *Progress in polymer science*, 2005, **30**, 10-37.
20. A. Kumar, R. Singh, S. P. Gopinathan and A. Kumar, *Chemical Communications*, 2012, **48**, 4905-4907.

21. J. Rhe and W. Knoll, *Journal of Macromolecular Science, Part C: Polymer Reviews*, 2002, **42**, 91-138.
22. Y.-H. Lee, W.-C. Yen, W.-F. Su and C.-A. Dai, *Soft Matter*, 2011, **7**, 10429-10442.
23. D. Neher, *Adv. Mater.*, 1995, **7**, 691-702.
24. T. K. Goh, S. N. Guntari, C. J. Ochs, A. Blencowe, D. Mertz, L. A. Connal, G. K. Such, G. G. Qiao and F. Caruso, *Small*, 2011, **7**, 2863-2867.
25. D. Mertz, C. J. Ochs, Z. Zhu, L. Lee, S. N. Guntari, G. K. Such, T. K. Goh, L. A. Connal, A. Blencowe, G. G. Qiao and F. Caruso, *Chem. Commun.*, 2011, **47**, 12601-12603.
26. E. H. H. Wong, S. N. Guntari, A. Blencowe, M. P. van Koeverden, F. Caruso and G. G. Qiao, *ACS Macro Letters*, 2012, **1**, 1020-1023.
27. E. H. H. Wong, M. P. van Koeverden, E. Nam, S. N. Guntari, S. H. Wibowo, A. Blencowe, F. Caruso and G. G. Qiao, *Macromolecules*, 2013, **46**, 7789-7796.
28. C. W. Bielawski and R. H. Grubbs, *Prog. Polym. Sci.*, 2007, **32**, 1-29.
29. M. Kamigaito, T. Ando and M. Sawamoto, *Chem. Rev.*, 2001, **101**, 3689-3746.
30. K. Matyjaszewski and J. Xia, *Chem. Rev.*, 2001, **101**, 2921-2990.
31. T. Otsu and A. Matsumoto, in *Microencapsulation Microgels Iniferters*, eds. S. DiMari, W. Funke, M. A. Haralson, D. Hunkeler, B. Joos-Mller, A. Matsumoto, O. Okay, T. Otsu, A. C. Powers, A. Prokop, T. G. Wang and R. R. Whitesell, Springer Berlin Heidelberg, 1998, vol. 136, ch. 3, pp. 75-137.
32. S. B. Rahane and A. T. Metters, *Macromolecules*, 2006, **39**, 8987-8991.
33. S. N. Guntari, A. C. H. Khin, E. H. H. Wong, T. K. Goh, A. Blencowe, F. Caruso and G. G. Qiao, *Adv. Funct. Mater.*, 2013, **23**, 5159-5166.
34. S. N. Guntari, E. H. H. Wong, T. K. Goh, R. Chandrawati, A. Blencowe, F. Caruso and G. G. Qiao, *Biomacromolecules*, 2013, **14**, 2477-2483.
35. S. N. Guntari, T. K. Goh, A. Blencowe, E. H. H. Wong, F. Caruso and G. G. Qiao, *Polymer Chemistry*, 2013, **4**, 68-75.
36. M. Lanzi, P. Costa-Bizzarri, C. Della-Casa, L. Paganin and A. Fraleoni, *Polymer*, 2003, **44**, 535-545.
37. R. H. Lohwasser and M. Thelakkat, *Macromolecules*, 2011, **44**, 3388-3397.
38. J. W. Bartels, P. M. Imbesi, J. A. Finlay, C. Fidge, J. Ma, J. E. Seppala, A. M. Nystrom, M. E. Mackay, J. A. Callow, M. E. Callow and K. L. Wooley, *ACS Applied Materials & Interfaces*, 2011, **3**, 2118-2129.
39. L. Kwisnek, M. Kaushik, C. E. Hoyle and S. Nazarenko, *Macromolecules*, 2010, **43**, 3859-3867.
40. C. Slugovc, *Macromol. Rapid Commun.*, 2004, **25**, 1283-1297.
41. S. R. White, N. Sottos, P. Geubelle, J. Moore, M. R. Kessler, S. Sriram, E. Brown and S. Viswanathan, *Nature*, 2001, **409**, 794-797.
42. M. Kessler, N. Sottos and S. White, *Composites Part A: applied science and manufacturing*, 2003, **34**, 743-753.
43. R. Simons, S. N. Guntari, T. K. Goh, G. G. Qiao and S. A. Bateman, *Journal of Polymer Science Part A: Polymer Chemistry*, 2012, **50**, 89-97.
44. M. S. Sanford, J. A. Love and R. H. Grubbs, *Organometallics*, 2001, **20**, 5314-5318.
45. Y. Kim, S. A. Choulis, J. Nelson, D. D. Bradley, S. Cook and J. R. Durrant, *Appl. Phys. Lett.*, 2005, **86**, 063502.
46. G. Jiang, R. Ponnampati, R. Pernites, M. J. Felipe, R. Advincula, *Macromolecules*, 2010, **43**, 10262-10274.
47. V. Senkovskyy, N. Khanduyeva, H. Komber, U. Oertel, M. Stamm, D. Kuckling, A. Kiriy, *J. Am. Chem. Soc.*, 2007, **129**, 6626-6632.



## TOC Abstract

The formation of cross-linked polymer films, with tunable thickness, proceeds directionally from the substrate surface by controlled polymerization in the solid state.

## TOC Figure

